

Energy loss of degrader in SC200 proton therapy facility

Feng Jiang^{1,2} · Yun-Tao Song^{1,2} · Jin-Xing Zheng^{1,2} · Xian-Hu Zeng^{1,2} · Peng-Yu Wang^{1,2} · Jun-Sheng Zhang^{1,2} · Wu-Quan Zhang¹

Received: 25 December 2017 / Revised: 21 April 2018 / Accepted: 13 May 2018 / Published online: 2 January 2019
© China Science Publishing & Media Ltd. (Science Press), Shanghai Institute of Applied Physics, the Chinese Academy of Sciences, Chinese Nuclear Society and Springer Nature Singapore Pte Ltd. 2019

Abstract The proton beam energy determines the range of particles and thus where the dose is deposited. According to the depth of tumors, an energy degrader is needed to modulate the proton beam energy in proton therapy facilities based on cyclotrons, because the energy of beam extracted from the cyclotron is fixed. The energy loss was simulated for the graphite degrader used in the beamline at the superconducting cyclotron of 200 MeV in Hefei (SC200). After adjusting the mean excitation energy of the graphite used in the degrader to 76 eV, we observed an accurate match between the simulations and measurements. We also simulated the energy spread of the degraded beam and the transmission of the degrader using theoretical formulae. The results agree well with the Monte Carlo simulation.

Keywords Degradation · Energy loss · Mean excitation energy · Energy spread · Transmission

1 Introduction

Since 1946, when R. Wilson revealed the advantageous dose distributions of protons, it has been shown that energetic protons can be useful for cancer therapy applications. Proton depth dose distributions are characterized by a relatively low dose at shallow depths, a peak near the end of the proton range, and then a rapid falloff. The peak is called the Bragg peak, as it was discovered by William Henry Bragg in 1903 [1]. Proton therapy facilities can deliver a high dose of ionizing radiation to a deep-seated tumor while not exceeding the tolerance dose of the intervening normal tissue and delivering nearly no dose to normal tissues beyond the tumor [2, 3].

The SC200 proton therapy facility (superconducting cyclotron of 200 MeV in Hefei, China) consists of a 200 MeV superconducting cyclotron, whose maximum beam intensity is approximately 400 nA, and a beamline that guides the beam to two treatment rooms, gantry treatment room and fixed beam treatment room [4, 5]. The beam energy is modulated using a degrader, which is inserted into the beam trajectory. The degrader can reduce the beam energy from 200 MeV to a value specified by the treatment planning, which varies at SC200 in the range of 70–190 MeV. The beam intensity of the degraded proton beam at the entrances of the treatment rooms depends strongly on the beam degrading process. The minimum transmission is obtained at 70 MeV, owing to the increase in the beam emittance caused by the multiple scattering that occurs when the proton beam is degraded. The increase in the energy spread, which must be limited in order to reduce the distal falloff of the Bragg peak, affects the transmission.

This work was supported in part by the National Natural Science Foundation of China (No. 51525703).

✉ Feng Jiang
jfeng@ipp.ac.cn

¹ Institute of Plasma Physics, Chinese Academy of Sciences, Hefei 230031, China

² University of Science and Technology of China, Hefei 230026, China

Some proton therapy facilities with a high primary beam energy degrade the beam energy in two steps for higher transmission. First, the beam energy is degraded to approximately 150 MeV in the beamline. Then, another degrader in the treatment room degrades the energy to the required energy. However, this is disadvantageous for treatments that require a sharp distal falloff of the Bragg peak. On the other hand, this method is very attractive for pencil beam scanning facilities. The larger distal falloff can reduce the number of scanning layers and the treatment time [6]. In SC200, the beam must be controlled over the full available range. Thus, there is only one degrader in SC200, and detailed information about the degrading process is required.

We do not aim for a universal theory that can solve all problems regarding protons passing through materials but rather for a set of equations allowing a degrader to be designed for a proton therapy facility. Moreover, we want to predict the transmission and properties of the beam, similar to the result of Monte Carlo program.

In this study, we investigated the energy loss and beam loss of the degrader using a theoretical calculation method. All of the programs were developed and executed in MATLAB. Then, we used several Monte Carlo codes to simulate the process of protons passing through the degrader. Herein, we present the experimental results to verify the rationality of the physical model.

2 Experimental section

2.1 Degrader description

The energy selection system (ESS) is an important subsystem of proton therapy facilities based on cyclotrons. This subsystem is necessary in proton therapy, as the beam energy extracted from the cyclotron is fixed and the required energy of treatment plans varies according to the depth of tumors. The ESS can adjust the energy and other properties of the extracted beam in accordance with the requirement of the treatment plan [7]. A typical ESS often includes a degrader, collimators, slits, quadrupole magnets, bending magnets, correction magnets, vacuum equipment, and beam diagnostic equipment [8–10].

The beam extracted from the SC200 cyclotron is focused at the degrader, by passing it through four quadrupole magnets. A double waist, in the horizontal and vertical directions, is formed in the degrader by a special design of beam optics, for minimizing the emittance after the degrader and enhancing the transmission of the ESS. Before the degrader, there is a “control point” to monitor the parameters of the extracted beam, including a current monitor placed permanently in the beam trajectory, a profile monitor, and a beam stopper, which is inserted into the beam when necessary. After the “control point,” collimator 1 is mainly used for reducing the influence of stray particles. The layout of ESS in SC200 was shown in Fig. 1.

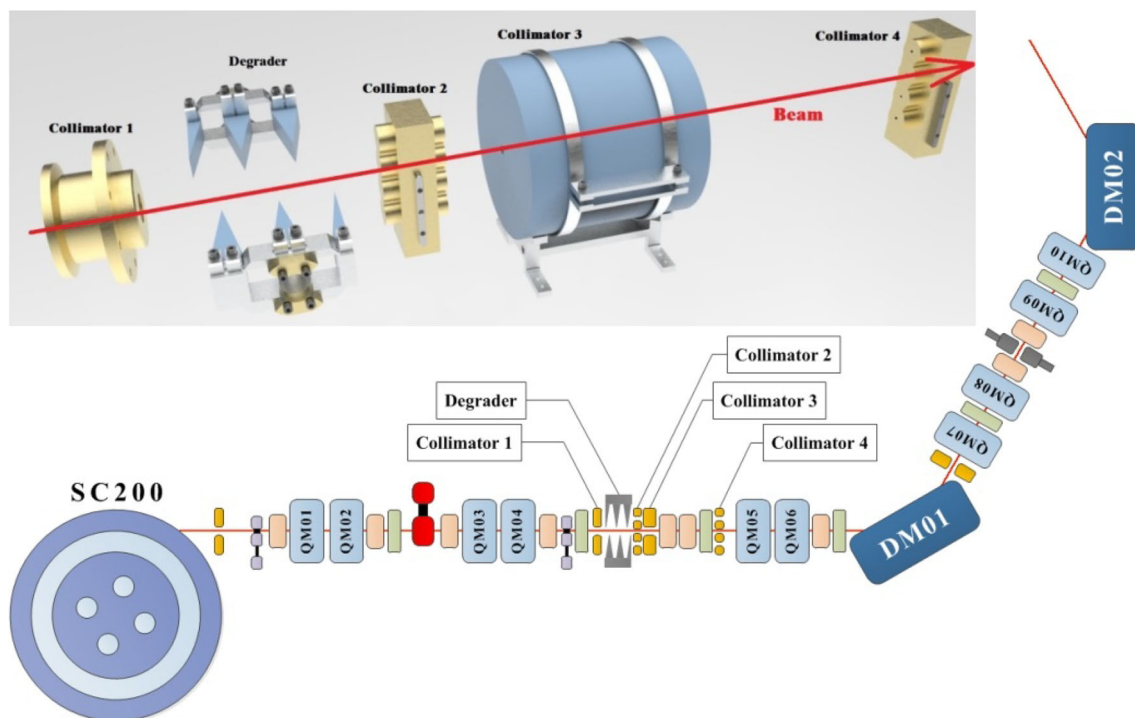


Fig. 1 (Color online) Schematic of the degrader and part of the ESS in SC200

The degrader consists of two parts, which are placed at the left and right sides of the beam. Each part has several full and half wedges, and the mid-plane of the degrader is the same as beam. This design of wedges can significantly reduce the time of degrader movement, ensuring a change time of < 2 s/layer. The wedges are made of high-density graphite ($\rho = 1.84 \pm 0.005$ g/cm³) and fixed on an aluminum base platform. On the base platform, we designed a water-cooled brass connection to remove heat from the wedges, which is caused by energy loss. Two servomotors are used to drive the wedges, which adjust the overlap of the degrader. These servomotors have very high control precision, along with a grating scale to verify their correct setting. To obtain a uniform thickness of the degrader, the entrance and exit of the degrader are parallel to each other and perpendicular to the axis of beam.

After the degrader, the beam passes through three collimators in sequence. The first and the third collimators are made of brass, have different cone apertures, and define the acceptable emittance for the downstream beamline. According to the requirement of the gantry and design of the downstream beamline, all of these apertures are circular for obtaining a round beam at the “control point” before the gantry. The first collimator defines the cross-sectional size of the degraded beam. The second collimator, which is very close to the first one, is made of graphite for absorbing stray particles. The third collimator defines the maximum scattering angle. This system of collimators controls the emittance in the range of $< 16\pi$ mm mrad, owing to the acceptance of the gantry.

Next are six quadruple magnets and two bending magnets, forming an achromatic system. The beam waist in the horizontal direction is designed at the center of the two bending magnets. At this location, the function between the envelope curve and the momentum spread is maximized (28 mm/% ΔP), and the momentum slit is placed here. The momentum spread of the transported beam can be selected by a slit with two servomotors in the horizontal directions. The maximum momentum spread is $\pm 1.2\%$. A momentum spread of $\pm 0.6\%$ is used for the gantry, to obtain a spot whose full width at half maximum is 4–10 mm at the isocenter.

2.2 Ionization energy loss calculation

To ensure that all of the beam is degraded, the width of the degrader overlap should be greater than the diameter of the beam. This method can avoid the uncertainty of the degraded distribution, owing to the statistical fluctuation that arises when a proton passes through a slice. On the other hand, this affects the available range of the beam

energy. The kinematic maximum possible electron recoil kinetic energy is given as

$$T_{\max} = \frac{2m_e c^2 \beta^2 \gamma^2}{1 + (m_e/M)^2 + 2(m_e/M) \cdot \gamma}, \tag{1}$$

where m_e is the mass of the electron, c is the speed of light, β is the ratio of the proton speed to light speed, $\gamma = (E + E_0)/E_0$, E_0 is the particle’s rest energy, E is the kinetic energy, and M is the mass of the projectile.

According to the definition of a “thick” medium, the average ionization energy loss in thickness δx should be defined by

$$\left(\frac{dE}{dx}\right) \delta x > T_{\max}. \tag{2}$$

The distribution of the degraded energy passed through a “thick” medium should be similar to a Gaussian distribution, and that for a “thin” medium should be similar to a Landau distribution. For a 200-MeV beam, the threshold between “thick” and “thin” is approximately 2.04 g/cm². In SC200, the minimum width of the overlap is approximately 13 mm, and the thickness of graphite is approximately 12 mm, allowing a degradation of an incident 200-MeV proton beam to the range of 70–191 MeV.

We use the Bethe–Bloch formula for the energy loss and range calculation [11–14]. The energy loss due to only ionization is given by

$$-\frac{dE}{dx} = -KZ_1^2 \rho \frac{Z_2}{A_2} \frac{1}{\beta^2} \left(\frac{1}{2} \ln \frac{2m_e c^2 \beta^2 \gamma^2}{I^2} T_{\max} - \beta^2 - \frac{C}{Z} - \frac{\delta}{2} \right), \tag{3}$$

where K is a constant equal to 0.3071; Z_1 is the charge of the incident particle (in units of e); ρ is the density of the degrader material; Z_2 and A_2 are the atomic number and mass of the target atom, respectively; I is the mean excitation energy; δ is the density effect correction; and C is the shell correction.

If the degrader is made of a compound material, the energy loss should be calculated for each component with relevant density:

$$-\frac{dE}{dx} = -KZ_1^2 \frac{1}{\beta^2} \sum_k \rho_k \frac{Z_{2k}}{A_{2k}} \left(\frac{1}{2} \ln \frac{2m_e c^2 \beta^2 \gamma^2}{I_k^2} T_{\max} - \beta^2 - \frac{C_k}{Z} - \frac{\delta_k}{2} \right). \tag{4}$$

The range of protons with the incident kinetic energy E_0 in materials is defined by

$$R(E_0) = \int_0^{E_0} \frac{dE}{|dE/dx|}. \tag{5}$$

The resulting range was obtained by integrating Eq. (3) via the Runge–Kutta method. We calculated the proton

range for several materials, including pure and compound materials.

2.3 Energy spread calculation

The process of passing a beam through the degrader material has obvious randomness, which incurs fluctuation of the energy loss. This means that a monoenergetic beam passing through degrader material will yield an energy spread (or momentum spread). This spread and the final energy are defined by the initial energy of the incident beam and the thickness of the degrader material, which are nonlinear [15–17].

In combination with the stochastic process, the energy spread should be defined by

$$\sigma_{E_{\text{final}}}^2 = \left(\frac{dE_{\text{final}}/dx}{dE_{\text{initial}}/dx} \right)^2 \left[\sigma_{E_{\text{initial}}}^2 + \left(\frac{dE_{\text{initial}}}{dx} \right)^2 \int_{E_{\text{initial}}}^{E_{\text{final}}} \frac{N(E)}{M(E)^3} dE \right], \tag{6}$$

$$N(E) = Km_e c^2 \rho \frac{Z_2}{A_2} (1 - \beta^2/2) \gamma^2, \tag{7}$$

where $M(E)$ is the mean ionization energy loss, and $N(E)$ is the stochastic energy spread for thin targets, which depends on the energy. According to the aforementioned theories and methods, we wrote the calculation programs using MATLAB.

2.4 Proton–nucleus collision model

When the proton beam passes through the degrader, the number of emerging protons undergoes exponential decay owing to the inelastic collision between the proton and nucleus. The proton–nucleus collision is a special case of the nucleus–nucleus collision. These parameters of the collision system are associated with the physics process. In general, Coulomb interaction plays a leading role at lower energies, and Pauli blocking has more influence at higher energies.

For two colliding ions, the total cross section σ_T equals the reaction cross section σ_R plus the elastic cross section σ_e . The empirical models often approximate the Bradt–Peters form. In addition, the effect of the Coulomb interaction should be considered at low energies. Tripathi [18] proposed the following model for calculating the reaction cross section:

$$\sigma_R = \pi r_0^2 \left(A_1^{1/3} + A_2^{1/3} + \delta_E \right)^2 \left(1 - \frac{B}{E_{\text{cm}}} \right), \tag{8}$$

where r_0 is a constant not dependent on the energy, A_1 is the mass of the incident particle, E_{cm} is the colliding center of mass energy, and B is the Coulomb interaction barrier, which depends on the energy. More importantly, the study

provided a good approximation for proton–nucleus collisions. Because of the small compression effect for proton–nucleus collisions, a coefficient D that is related to the density of the colliding system is defined as a constant to be a very good match at all energies.

The proportion of the proton beam in the entire decay process is determined by

$$N = N_0 e^{-\sum \rho/\lambda}, \tag{9}$$

where N and N_0 represent the numbers of protons in the degraded and incident beams, respectively, and λ is the mean free path.

2.5 Experiment

Two graphite triple wedge blocks (Fig. 2a) were produced by the Institute of Solid State Physics. The average grain size of this isostatic graphite is only 7 μm , and the bulk density is approximately 1.84 g/cm^3 . These two blocks were mounted on an aluminum frame with two servomotors for driving them. The thickness of graphite can reach 130 mm, which is suitable for SC200.

As the transmission depends strongly on the energy, it is important to set the degraded beam energy with high accuracy. We placed the graphite blocks on the treatment bed of Gantry 2 at the Paul Scherrer Institute (PSI) and aligned them carefully in order to make the beam entrance perpendicular to the beam. The energy of the “initial beam,” before these blocks, was divided into 116 points from 70 to 230 MeV by adjusting the beamline and was measured by monitors in the nozzle. The thickness of the graphite blocks was set at 15 positions (intervals of 10 mm from 6 mm to 126, 0, and 130 mm). We used a multi-layer ionization chamber (MLIC, Fig. 2b) to measure the beam energy after the graphite blocks. The measurement range of this MLIC was approximately 277-mm water phantom, with an error of approximately 1 mm. The beam currents before and after the graphite blocks were measured to obtain the transmission by using monitors.

3 Results and Discussion

3.1 Mean excitation energy of graphite

In the calculation of the energy loss in the degrader, the most important parameter is the mean excitation energy. In earlier literature, this parameter is often given by the experimental formula $I = I_0 Z$. The coefficient I_0 differs among various sources. It is often assumed to be 13 eV, and the coefficient of light atom is slightly lower—closer to 10 eV. Except for hydrogen, the mean excitation energy of

Fig. 2 (Color online) Experiment of degrader energy loss. **a** Graphite blocks, **b** MLIC

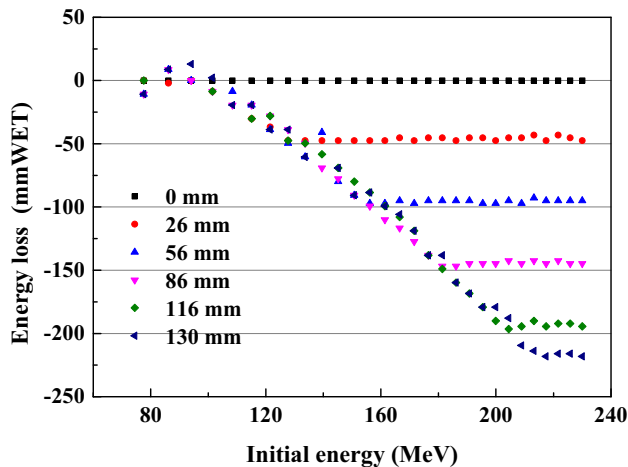
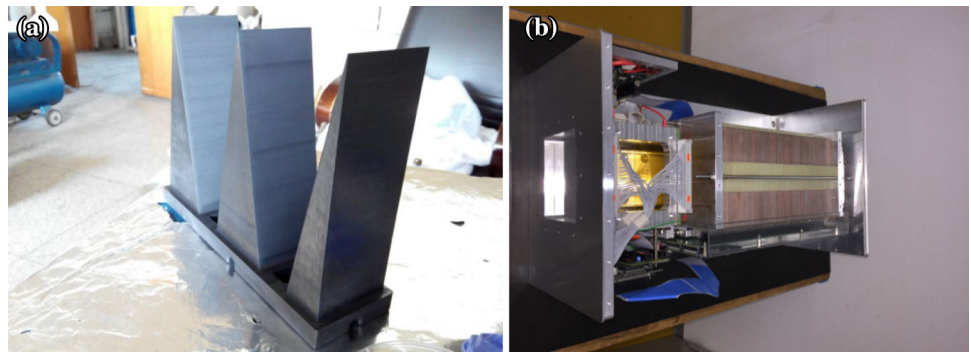


Fig. 3 (Color online) Energy loss under different initial energies in the experiment

each material should be measured experimentally. In the web database PSTAR of the National Institute of Standards and Technology (NIST), which calculates stopping powers, ranges, and related quantities for protons, the material properties of two kinds of graphite are given. One is amorphous carbon, which has a density close to 2.00 g/cm^3 and mean excitation energy of 81 eV. The other is graphite, which has a density of approximately 1.70 g/cm^3 and mean excitation energy of 78 eV.

We set up an experiment to study the mean excitation energy of graphite, which is chosen to make the degrader. The results in Fig. 3 show that the functions of the energy loss and graphite thickness under different “initial beam” energies agree with the linear rule. This reveals that the graphite blocks are uniform.

In addition, we used different I values to simulate the energy loss of the degrader, from 60 to 100 eV. According to the percentage difference between the degraded energy from the measurement and simulation, we obtained a function of the degrader length for different mean excitation energies of graphite, as shown in Fig. 4. The experimental results indicate that 76 eV is the most suitable.

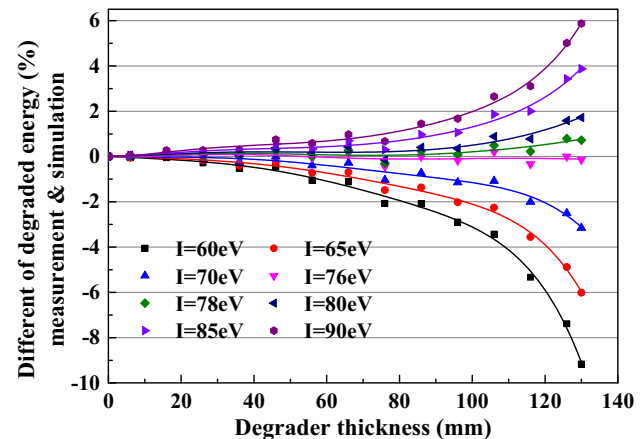


Fig. 4 (Color online) Difference between the measurement and simulation

3.2 Ionization energy loss of degrader

We calculated the ionization energy loss of a proton beam passed through the degrader using Eq. (3). For the interaction between incident protons and carbon atoms, three kinds of corrections are considered: relativistic correction, shell correction, and density effect correction. The relativistic correction begins to take effect at approximately 100 MeV and plays an important role after several GeV [19]. At 200 MeV, the relativistic correction is $< 1\%$. This is equal to the density effect correction, which arises around 300 MeV and increases to 5% at 1.5 GeV. However, the shell correction differs. It is more important at a lower energy. When the incident energy is $< 4 \text{ MeV}$, the shell correction is approximately 2%. It is almost not working above 20 MeV, as shown in Fig. 5.

As shown in Fig. 6, the stopping power of different materials for the proton beam is similar. At the zone of $\beta\gamma = 3-4$, the stopping power is minimized, called minimum ionizing particles (MIPs). In SC200, the maximum $\beta\gamma$ is < 0.7 . That is, the stopping power depends linearly on $1/\beta^2$.

The energy loss in the degrader under a 200-MeV “initial beam” is shown in Fig. 7. We compared the results

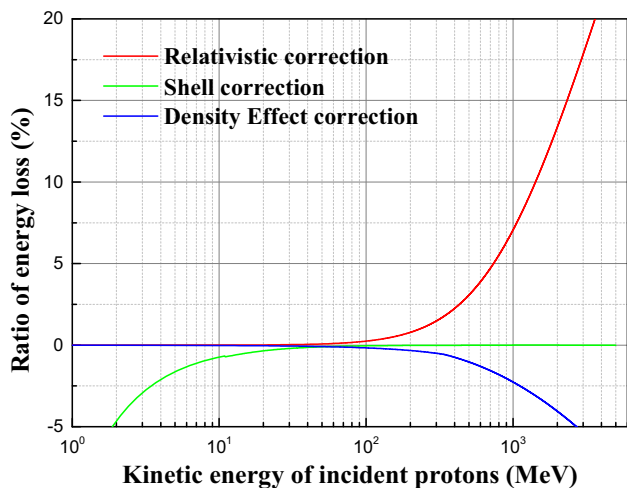


Fig. 5 (Color online) Corrections of the Bethe–Bloch formula with respect to the incident energy

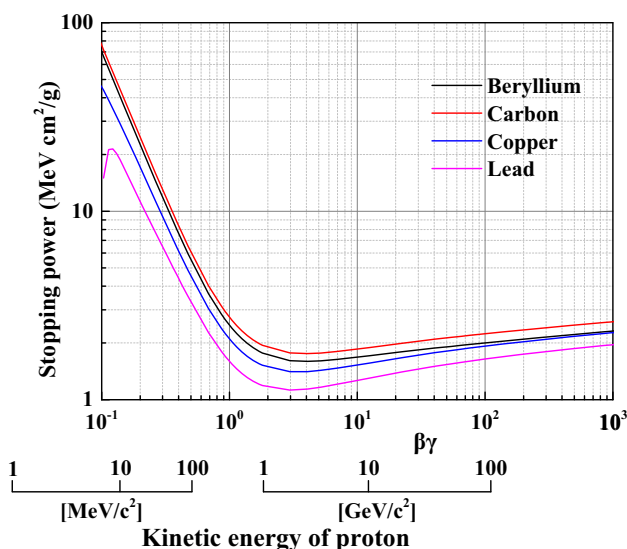


Fig. 6 (Color online) Stopping power of different materials for protons

of Monte Carlo simulation [20, 21] with theoretical results and measurement data. The error is $< 1.354\%$ between the two simulation methods and is $< 2.263\%$ between the calculation and experiment. According to the results of the error analysis, the errors between the calculation results and the experiment data mainly result from the equivalent thickness of the monitors in the MLIC (each monitor is equivalent to 2.2 mm water).

3.3 Energy spread of degraded beam

We used Eq. (6) to calculate the energy spread after the degrader. First, the initial beam with the energy spread in the Gaussian distribution was divided into monochrome

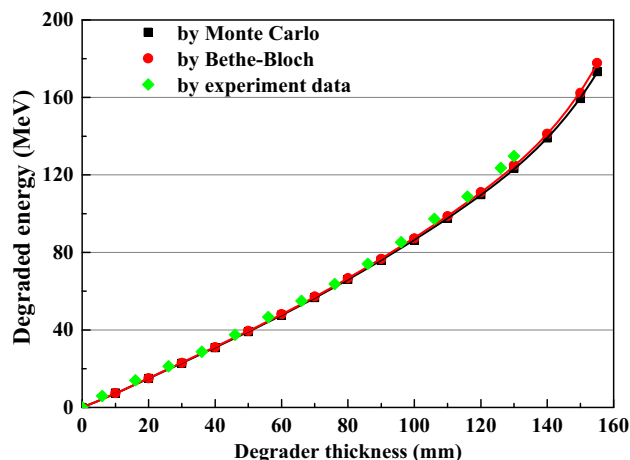


Fig. 7 (Color online) Energy loss calculation for the degrader made of graphite

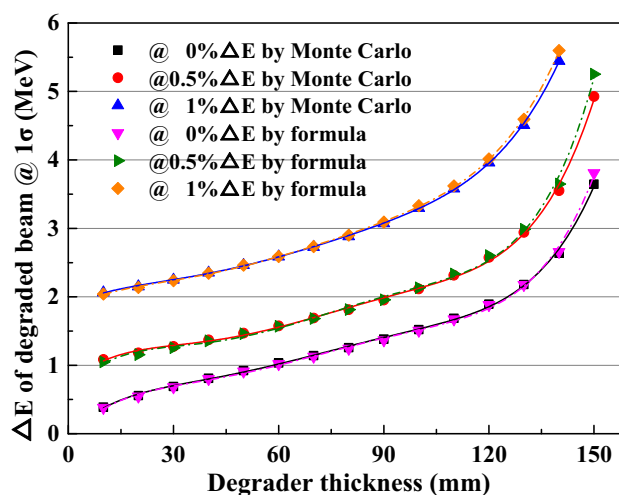


Fig. 8 (Color online) Comparison of the energy spread after the degrader

beams with different weights. Second, every monochrome beam was calculated for the distribution of the degraded beam. The final result was obtained using multi-Gaussian superimposition.

As shown in Fig. 8, the calculation and simulation results were compared and agreed well. When the thickness is relatively small, the formula results are slightly lower than the Monte Carlo results, owing to the several δ electrons with high energy. The distribution has a long tail in the high energy loss zone and is more similar to the Landau distribution than to the Gaussian distribution. Figure 9 shows the standard deviation of the degraded beam with an initial beam in the 0–1.0% energy spread. Obviously, the minus error bars are longer than plus error bars, which is caused by the tail at a low energy. A typical energy spread of the degraded beam is shown in Fig. 10.

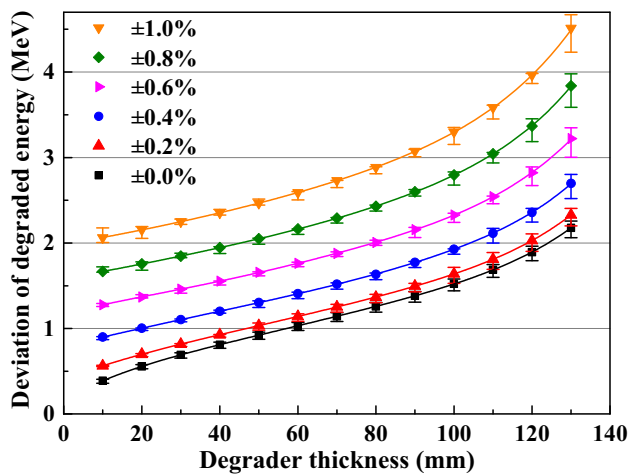


Fig. 9 (Color online) Standard deviation of the energy after the degrader with different initial spreads

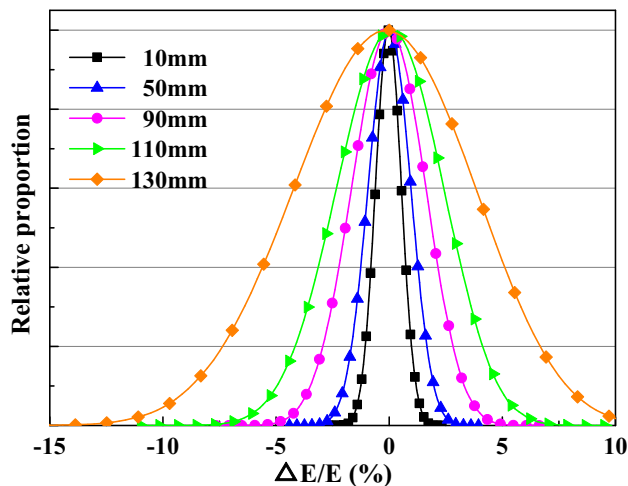


Fig. 10 (Color online) Energy spread after the degrader with $\pm 0.5\%$ initial spread (1σ)

3.4 Transmission of degrader

According to the empirical formula for the proton–nucleus collision, we calculated the reaction cross section of two materials that are typically used to make degraders: beryllium and carbon. We compared the results with experimental data reported by Tripathi [18]. The comparison is presented in Fig. 11.

The agreement between the empirical formula and the experiment is very good. Obviously, the cross sections are affected by the Coulomb interaction at the lower energy end. Pauli blocking effects become increasingly important at a high energy.

For confirming the loss of beam current when protons pass through degrader, we calculated the transmission of the graphite degrader using the cross–section function and compared the result with Monte Carlo simulation and

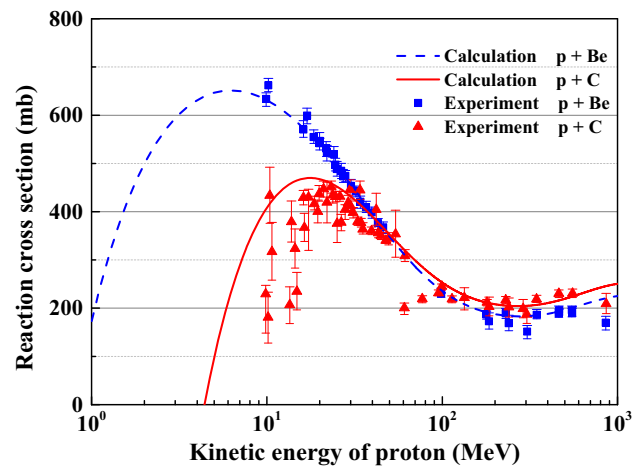


Fig. 11 (Color online) Reaction cross sections for the proton–nucleus collisions

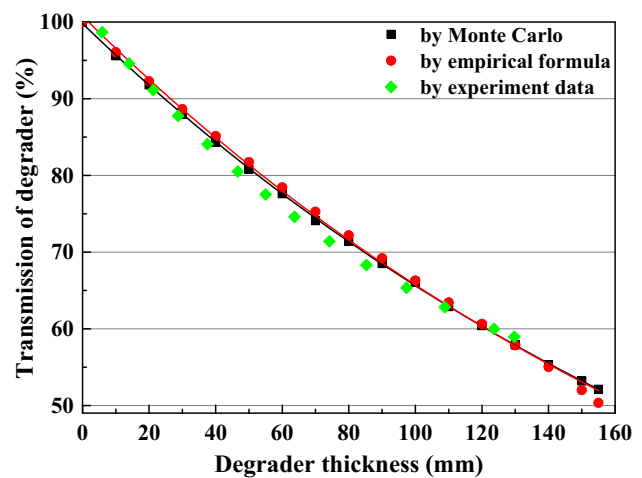


Fig. 12 (Color online) Transmission of the degrader made of graphite

experimental data, as shown in Fig. 12. The transmission error is $< 1.593\%$ between the two simulation methods and $< 1.719\%$ between the calculation and experiment.

4 Conclusion

We developed a degrader simulation program to calculate the energy loss and beam loss for protons passing through a degrader, according to theoretical formulae and empirical formulae. The results of the simulation of the degrader in the SC200 proton therapy facility exhibit very good agreement with experimental measurements and Monte Carlo simulation results. Thus, the rationality of the physical model is verified.

After the mean excitation energy of the graphite degrader used in SC200 is adjusted, the energy loss

calculation for the degrader reproduces the measured value within 2.263% at 70–200 MeV. This means that the standard material properties are not accurate enough for high-accuracy simulations. All of the properties used in nuclear stopping simulation should be measured by experiments. According to an analysis of the main component in the ionization energy loss analysis, we defined the scope of each component and calculated the stopping power of several common materials.

Finally, we constructed the physical model of the proton–nucleus collision using the approximate formulae. The transmission of the degrader closely approximated that of the Monte Carlo simulation, with an error of < 1.593%.

Acknowledgements The authors are grateful for the financial support from Hefei CAS Ion Medical and Technical Devices Co., Ltd.

References

1. J.M. Slater, O.J. Archambeau, D.W. Miller et al., The proton treatment center at Loma Linda University Medical Center: rationale for and description of its development. *Int. J. Radiat. Oncol. Biol. Phys.* **22**, 383–389 (1992). [https://doi.org/10.1016/0360-3016\(92\)90058-p](https://doi.org/10.1016/0360-3016(92)90058-p)
2. W.P. Jones, G.P.A. Berg, Design of a beam transport system for a proton radiation therapy facility, in *Particle Accelerator Conference, 1999. Proceedings of the. IEEE*, vol. 4, 1999, pp. 2519–2521. <https://doi.org/10.1109/pac.1999.792752>
3. J.B. Flanz, F. Gerardi, E.L. Hubbard, Design considerations for a proton therapy beamline with an energy degrader, in *Fourteenth International Conference on the Application of Accelerators in Research & Industry* (American Institute of Physics, 1997), pp. 1257–1260. <https://doi.org/10.1063/1.52693>
4. G. Karamysheva, Y. Bi, G. Chen, et al., Compact superconducting cyclotron SC200 for proton therapy, in *Proceedings of Cyclotrons 2016*, Zurich, Switzerland, September 2016
5. X.H. Zeng, J.X. Zheng, Y.T. Song et al., Beam optics study for energy selection system of SC200 superconducting proton cyclotron. *Nucl. Sci. Tech.* **29**, 134 (2018). <https://doi.org/10.1007/s41365-018-0462-5>
6. E. Pedroni, R. Bearpark, T. Böhringer et al., The PSI Gantry 2: a second generation proton scanning gantry. *Med. Phys.* **14**, 25–34 (2004). <https://doi.org/10.1078/0939-3889-00194>
7. M.J. van Goethem, R. van der Meer, H.W. Reist et al., Geant4 simulations of proton beam transport through a carbon or beryllium degrader and following a beam line. *Phys. Med. Biol.* **54**, 5831–5846 (2009). <https://doi.org/10.1088/0031-9155/54/19/011>
8. F. Stichelbaut, Y. Jongen, Properties of an energy degrader for light ions. **4**, 272–275 (2014). <https://doi.org/10.15669/pnst.4.272>
9. E.W. Cascio, S. Sarkar, A continuously variable water beam degrader for the radiation test beamline at the Francis H. Burr Proton Therapy Center, in *2007 IEEE Radiation Effects Data Workshop*, 2007, pp. 30–33. <https://doi.org/10.1109/redw.2007.4342536>
10. J.A. Brennsæter, *The Influence of the Energy Degrader Material for a Therapeutic Proton Beam*, 2015
11. M.J. Berger, et al., Stopping powers and ranges for protons and alpha particles. *J. Int. Comm. Radiat. Units Meas.* (1993). <https://doi.org/10.1093/jicru/os25.2.Report49>
12. D.E. Groom, Energy loss in matter by heavy particles. Particle Data Group Notes, PDG-93-06
13. D.E. Groom, S.R. Klein, Passage of particles through matter. *Eur. Phys. J. C* **15**, 163–173 (2000). <https://doi.org/10.1007/bf02683419>
14. M. Behar, C.D. Denton, R.C. Fadanelli et al., Experimental and theoretical determination of the stopping power of ZrO₂ films for protons and α -particles. *Eur. Phys. J. D* **59**, 209–213 (2010). <https://doi.org/10.1140/epjd/e2010-00164-x>
15. C.C. Montanari, J.E. Miraglia, S. Heredia-Avalos et al., Calculation of energy-loss straggling of C, Al, Si, and Cu for fast H, He, and Li ions. *Phys. Rev. A* **75**, 441–445 (2007). <https://doi.org/10.1103/PhysRevA.75.022903>
16. Y. Kido, T. Hioki, Measurements of energy loss and straggling for fast H⁺ in metals and their compounds by means of a nuclear resonant reaction. *Phys. Rev. B* **27**, 2667–2673 (1983). <https://doi.org/10.1103/physrevb.27.2667>
17. M. Behar, R.C. Fadanelli, I. Abril et al., Energy-loss straggling study of proton and alpha-particle beams incident onto ZrO₂, and Al₂O₃ films. *Eur. Phys. J. D* **64**, 297–301 (2011). <https://doi.org/10.1140/epjd/e2011-20352-4>
18. R.K. Tripathi, F.A. Cucinotta, J.W. Wilson, Universal parameterization of absorption cross sections. *Nucl. Instrum. Methods B.* **117**, 347 (1996). [https://doi.org/10.1016/0168-583x\(96\)00331-x](https://doi.org/10.1016/0168-583x(96)00331-x)
19. H. Paul, A comparison of recent stopping power tables for light and medium-heavy ions with experimental data, and applications to radiotherapy dosimetry. *Nucl. Instrum. Methods* **247**, 166–172 (2006). <https://doi.org/10.1016/j.nimb.2006.01.059>
20. T. Aso, A. Kimura, S. Tanaka et al., Verification of the dose distributions with GEANT4 simulation for proton therapy. *IEEE Trans. Nucl. Sci.* **52**, 896–901 (2005). <https://doi.org/10.1109/nssmic.2004.1462685>
21. H. Paganetti, H. Jiang, S.Y. Lee et al., Accurate Monte Carlo simulations for nozzle design, commissioning and quality assurance for a proton radiation therapy facility. *Med. Phys.* **31**, 2107 (2004). <https://doi.org/10.1118/1.1762792>